Conference Applications of Mathematics 2015, in honor of the birthday anniversaries of Ivo Babuška (90), Milan Práger (85), and Emil Vitásek (85)
J. Brandts, S. Korotov, M. Křížek, K. Segeth, J. Šístek, T. Vejchodský (Eds.)
Institute of Mathematics CAS, Prague 2015

A MULTI-SPACE ERROR ESTIMATION APPROACH FOR MESHFREE METHODS

Marcus Rüter[1], Jiun-Shyan Chen[2]

[1] Department of Civil and Environmental Engineering
University of California, Los Angeles, CA 90095, USA
marcus.ruter@ucla.edu
[2] Department of Structural Engineering
University of California, San Diego, La Jolla, CA 92093, USA
js-chen@ucsd.edu

Abstract: Error-controlled adaptive meshfree methods are presented for both global error measures, such as the energy norm, and goal-oriented error measures in terms of quantities of interest. The meshfree method chosen in this paper is the reproducing kernel particle method (RKPM), since it is based on a Galerkin scheme and therefore allows extensions of quality control approaches as already developed for the finite element method. Our approach of goal-oriented error estimation is based on the well-established technique using an auxiliary dual problem. To keep the formulation general and to add versatility, a multi-space approach is used, where the dual problem is solved numerically using a different approximation space than the one employed in the associated primal problem. This can be realized with meshfree methods at no additional cost. Possible merits of this multi-space approach are discussed and an illustrative numerical example is presented.

Keywords: reproducing kernel particle method (RKPM), meshfree methods, goal-oriented error estimation, dual problem

MSC: 65N15, 65N50, 74B05, 74R10

1. Introduction

In this paper, we confine our attention to error control of Galerkin-type meshfree methods, more specifically to error control of the reproducing kernel particle method (RKPM). From an error control point of view this has the advantage that error estimation techniques, as extensively developed for the finite element method, can generally be transferred to RKPM as they are both Galerkin methods.

Although meshfree methods offer several obvious advantages for *a posteriori* error control, the development of error estimators is surprisingly still in an early stage.

To date, the largest class of error estimators for meshfree methods constitutes of recovery-type error estimators. Mathematically more sound error estimators can be found in the class of residual-type error estimators. By construction, such error estimators have the virtue to offer error bounds. However, owing to several pessimistic inequalities that are usually used in their derivations, the error bounds of residual-type error estimators are typically not as sharp as the error approximations of recovery-type error estimators. Subclasses of this type of error estimation procedures constitute of explicit-type estimators, where the residual is used directly in the line of the pioneering works by Babuška & Rheinboldt [3, 4], and implicit-type estimators, where auxiliary local problems based on the residual are solved in the line of Bank & Weiser [6].

To the knowledge of the authors, in meshfree methods each of these subclasses currently consists of one representative. An explicit residual-type error estimator was developed by Duarte & Oden [8] for the meshfree method by the same authors, called *h-p* clouds. More recently, Vidal et al. [14] presented an implicit residual-type error estimator, where the auxiliary local problems are solved on patches of the integration cells so that no fluxes need to be taken into account. The authors are also the first ones who derived goal-oriented error estimators for meshfree methods.

In this paper, we follow Rüter & Chen [11] to add a new error estimator to the class of implicit residual-type error estimators for meshfree methods based on the finite element counterpart as introduced by Bank & Weiser [6] and further developed by Ainsworth & Oden [1] and others, see also Babuška & Strouboulis [5]. The error estimator presented in this paper is first derived for an energy-norm error control and is later extended to goal-oriented error estimation. It takes advantage of two key properties of meshfree methods. The first one is the high regularity of the meshfree solution which is reflected in a smooth stress field and thus in a smooth traction field. The second one is the independence of the particles from the integration cells which makes it possible to use different discretizations for the primal and for the dual problem, as used for the goal-oriented error estimator, at no additional cost. This multi-space approach thus bypasses the tedious transfer of discrete solutions from one mesh to the other as is required for mesh-based methods, such as the finite element method, as shown in Rüter et al. [12]. It is therefore tailored to meshfree methods and adds versatility and convenience to the goal-oriented error estimator proposed in this paper.

The paper is divided up as follows: in Section 2, the model problem of linear elasticity is presented. Furthermore, the meshfree method, RKPM, is introduced. Section 3 focuses on the derivation of a global implicit residual-type error estimator. In Section 4, the error estimator is extended to the case of goal-oriented error estimators where the error measure is given in terms of an arbitrary, user-defined quantity of interest. Thereby, emphasis is placed on the multi-space approach. The error estimator is then applied to a linear elastic fracture mechanics (LEFM) problem in Section 5. The paper concludes with Section 6, which summarizes the major findings achieved from theoretical and numerical points of view.

2. The model problem and its meshfree discretization

In this section, we briefly present the linear elasticity problem in its strong and weak forms. Furthermore, we show how a meshfree Galerkin method can be constructed based on reproducing kernel (RK) shape functions.

2.1. Strong and weak forms

We first introduce the elastic body which is given by the open, bounded domain $\Omega \subset \mathbb{R}^d$ with dimension $d \in \{1, 2, 3\}$. Its boundary $\Gamma = \partial\Omega$ consists of two disjoint parts $\Gamma_D \subset \Gamma$ and $\Gamma_N = \Gamma \setminus \bar{\Gamma}_D$, where, for simplicity, homogeneous Dirichlet and (generally inhomogeneous) Neumann boundary conditions are imposed, respectively.

The strong form of the elliptic and self-adjoint model problem of linear elasticity is to find the displacement field $\boldsymbol{u}$ such that the field equations

$$-\operatorname{div}\boldsymbol{\sigma}(\boldsymbol{u}) = \boldsymbol{f} \quad \text{in } \Omega \tag{1a}$$

$$\boldsymbol{\sigma} - \mathbb{C} : \boldsymbol{\varepsilon}(\boldsymbol{u}) = \boldsymbol{0} \quad \text{in } \Omega \tag{1b}$$

$$\boldsymbol{\varepsilon} - \boldsymbol{\nabla}^{\mathrm{sym}}\boldsymbol{u} = \boldsymbol{0} \quad \text{in } \Omega \tag{1c}$$

subjected to the boundary conditions

$$\boldsymbol{u} = \boldsymbol{0} \quad \text{on } \Gamma_D \tag{2a}$$

$$\boldsymbol{\sigma}(\boldsymbol{u}) \cdot \boldsymbol{n} = \bar{\boldsymbol{t}} \quad \text{on } \Gamma_N \tag{2b}$$

are fulfilled. In the above, $\boldsymbol{\sigma}$ denotes the stress tensor, $\boldsymbol{\varepsilon}$ is the strain tensor, and $\mathbb{C}$ is the elasticity tensor. Furthermore, on the right-hand sides of (1) and (2) we have prescribed body forces $\boldsymbol{f}$ and tractions $\bar{\boldsymbol{t}}$ that are assumed to be in the spaces $\boldsymbol{L}_2(\Omega)$ and $\boldsymbol{L}_2(\Gamma_N)$, respectively. Lastly, $\boldsymbol{n}$ denotes the unit outward normal.

In the classical weak formulation associated with (1) and (2) we seek for a solution $\boldsymbol{u}$ in the trial and test space $\mathcal{V}_0 = \{\boldsymbol{v} \in \boldsymbol{H}^1(\Omega)\,;\, \boldsymbol{v}|_{\Gamma_D} = \boldsymbol{0}\} \subset \mathcal{V} = \boldsymbol{H}^1(\Omega)$ such that

$$a(\boldsymbol{u}, \boldsymbol{v}) = F(\boldsymbol{v}) \quad \forall \boldsymbol{v} \in \mathcal{V}_0. \tag{3}$$

Here, a is a bilinear form defined on $\mathcal{V} \times \mathcal{V}$ as

$$a(\boldsymbol{u}, \boldsymbol{v}) = \int_\Omega \boldsymbol{\sigma}(\boldsymbol{u}) : \boldsymbol{\varepsilon}(\boldsymbol{v}) \, \mathrm{d}V \tag{4}$$

and F is a linear form defined on $\mathcal{V}$ as

$$F(\boldsymbol{v}) = \int_\Omega \boldsymbol{f} \cdot \boldsymbol{v} \, \mathrm{d}V + \int_{\Gamma_N} \bar{\boldsymbol{t}} \cdot \boldsymbol{v} \, \mathrm{d}A. \tag{5}$$

2.2. Reproducing kernel shape functions

In the associated meshfree Galerkin formulation of the weak form (3), we project (3) onto a suitable finite-dimensional subspace $\mathcal{V}_h \subset \mathcal{V}$ with

$$\mathcal{V}_h = \operatorname{span}\{\Psi_I\}_I^{n_P}, \tag{6}$$

where n_P is the number of particles $\boldsymbol{x}_I \in \bar{\Omega}$. A function $\boldsymbol{v}_h \in \mathcal{V}_h$ can then be expressed as

$$\boldsymbol{v}_h(\boldsymbol{x}) = \sum_{n_P} \Psi_I(\boldsymbol{x})\boldsymbol{v}_I \quad \forall \boldsymbol{x} \in \bar{\Omega}. \tag{7}$$

Here, $\boldsymbol{v}_I$ is a particle coefficient but, as opposed to the finite element method, in general not the value of $\boldsymbol{v}_h$ at particle $\boldsymbol{x}_I$, i.e. $\boldsymbol{v}_I \neq \boldsymbol{v}_h(\boldsymbol{x}_I)$, since, in general, the reproducing kernel (RK) shape functions Ψ_I do not possess the Kronecker-delta property (unlike the finite element shape functions), i.e. $\Psi_I(\boldsymbol{x}_J) \neq \delta_{IJ}$. Thus, Dirichlet boundary conditions cannot be satisfied by functions $\boldsymbol{v}_h \in \mathcal{V}_h$. As a consequence, it is obvious that, in general, $\mathcal{V}_h \not\subset \mathcal{V}_0$.

The meshfree RK shape function Ψ_I associated with a particle $\boldsymbol{x}_I$ takes the specific form

$$\Psi_I(\boldsymbol{x}) = \Phi(\boldsymbol{x} - \boldsymbol{x}_I)\boldsymbol{H}^T(\boldsymbol{0})\boldsymbol{M}^{-1}(\boldsymbol{x})\boldsymbol{H}(\boldsymbol{x} - \boldsymbol{x}_I) \tag{8}$$

with kernel function Φ, typically chosen as a cubic B-spline, vector of monomial basis functions $\boldsymbol{H}$, and the symmetric moment matrix

$$\boldsymbol{M}(\boldsymbol{x}) = \sum_{n_P} \Phi(\boldsymbol{x} - \boldsymbol{x}_I)\boldsymbol{H}(\boldsymbol{x} - \boldsymbol{x}_I)\boldsymbol{H}^T(\boldsymbol{x} - \boldsymbol{x}_I). \tag{9}$$

Note that since $\boldsymbol{M}$ needs to be invertible, the support of the kernel function Φ, i.e. $\operatorname{supp}\Phi$, needs to cover a sufficient amount of particles, see [7].

2.3. The reproducing kernel particle method

RKPM is a Galerkin method based on the RK shape functions as introduced in the previous section. As such, it is clear from the above that (homogeneous) Dirichlet boundary conditions on Γ_D are generally not fulfilled by the method. Without loss of generality, in this paper we make use of Nitsche's method to weakly impose the Dirichlet boundary conditions, see [10, 2], which leads to the following discrete problem associated with (3): find the RKPM solution $\boldsymbol{u}_h \in \mathcal{V}_h$ such that

$$a_h(\boldsymbol{u}_h, \boldsymbol{v}_h) = F(\boldsymbol{v}_h) \quad \forall \boldsymbol{v}_h \in \mathcal{V}_h. \tag{10}$$

Here, the discretization-dependent, symmetric bilinear form a_h is defined as

$$a_h(\boldsymbol{u}_h, \boldsymbol{v}_h) = a(\boldsymbol{u}_h, \boldsymbol{v}_h) - \int_{\Gamma_D} \boldsymbol{v}_h \cdot \boldsymbol{\sigma}(\boldsymbol{u}_h) \cdot \boldsymbol{n} \, \mathrm{d}A - \int_{\Gamma_D} \boldsymbol{u}_h \cdot \boldsymbol{\sigma}(\boldsymbol{v}_h) \cdot \boldsymbol{n} \, \mathrm{d}A + \frac{\beta}{h} \int_{\Gamma_D} \boldsymbol{u}_h \cdot \boldsymbol{v}_h \, \mathrm{d}A \tag{11}$$

with discretization parameter h and penalty parameter $\beta \in \mathbb{R}^+$ that takes the role of a stabilization parameter. Note that the right-hand side remains unchanged, since homogeneous boundary conditions are imposed on Γ_D.

3. Implicit energy norm residual-type error estimation

In what follows, we will derive an energy-norm error estimator of implicit residual type, which is based on a projected error residual equation to account for Nitsche's method and to get a symmetric form. The error estimator is established in terms of local forms of the projected error residual equation on each (Gauss) integration cell.

3.1. The error residual equation

The discretization error is defined in the usual way as $\boldsymbol{e} = \boldsymbol{u} - \boldsymbol{u}_h$. However, the error $\boldsymbol{e}$ as obtained by RKPM is an element of $\mathcal{V}_E = \{\boldsymbol{v} \in \boldsymbol{H}^1(\Omega)\,;\, \boldsymbol{v}|_{\Gamma_D} = \boldsymbol{e}|_{\Gamma_D}\} \subset \mathcal{V}$ rather than $\mathcal{V}_0$ as in mesh-based methods thanks to the Kronecker delta property of the mesh-based shape functions.

The starting point of our *a posteriori* error analysis will be the (extended) error residual equation

$$a(\boldsymbol{e}, \boldsymbol{v}) - \int_{\Gamma_D} \boldsymbol{v} \cdot \boldsymbol{\sigma}(\boldsymbol{e}) \cdot \boldsymbol{n} \, \mathrm{d}A = \hat{R}(\boldsymbol{v}) \quad \forall \boldsymbol{v} \in \mathcal{V}, \tag{12}$$

where the extended residual $\hat{R}$ is defined on $\mathcal{V}$ as

$$\hat{R}(\boldsymbol{v}) = F(\boldsymbol{v}) - a(\boldsymbol{u}_h, \boldsymbol{v}) + \int_{\Gamma_D} \boldsymbol{v} \cdot \boldsymbol{\sigma}(\boldsymbol{u}_h) \cdot \boldsymbol{n} \, \mathrm{d}A \tag{13a}$$

$$= \int_\Omega \boldsymbol{f} \cdot \boldsymbol{v} \, \mathrm{d}V + \int_{\Gamma_N} \bar{\boldsymbol{t}} \cdot \boldsymbol{v} \, \mathrm{d}A - \int_\Omega \boldsymbol{\sigma}(\boldsymbol{u}_h) : \boldsymbol{\varepsilon}(\boldsymbol{v}) \, \mathrm{d}V + \int_{\Gamma_D} \boldsymbol{t}_h \cdot \boldsymbol{v} \, \mathrm{d}A. \tag{13b}$$

Note that if $\boldsymbol{v}$ is chosen from $\mathcal{V}_0$, then (12) simplifies to the well-known equation $a(\boldsymbol{e}, \boldsymbol{v}) = R(\boldsymbol{v})$. Obviously, coercivity is an issue in (12). Therefore, and also to deal with the bilinear form a only, we propose to introduce a projection of the error in $\mathcal{V}_E$, denoted by $\hat{\boldsymbol{e}}$ and with the obvious property $\hat{\boldsymbol{e}}|_{\Gamma_D} = \boldsymbol{e}|_{\Gamma_D}$. This projection is defined via

$$a(\hat{\boldsymbol{e}}, \boldsymbol{v}) = a(\boldsymbol{e}, \boldsymbol{v}) - \int_{\Gamma_D} \boldsymbol{v} \cdot \boldsymbol{\sigma}(\boldsymbol{e}) \cdot \boldsymbol{n} \, \mathrm{d}A \quad \forall \boldsymbol{v} \in \mathcal{V} \tag{14}$$

and leads to the projected error residual equation

$$a(\hat{\boldsymbol{e}}, \boldsymbol{v}) = \hat{R}(\boldsymbol{v}) \quad \forall \boldsymbol{v} \in \mathcal{V} \tag{15}$$

with coercive bilinear form a. Using the discretization-dependent norm

$$\|\boldsymbol{v}\|^2_{\frac{1}{2},h} = \sum_{E \subset \Gamma_D} h_E^{-1} \|\boldsymbol{v}\|^2_{L_2(E)}, \tag{16}$$

with edge discretization parameter h_E and edge E, the Cauchy-Schwarz inequality, and an inverse estimate with positive constant C, it can be shown, see [11], that

$$|\!|\!| \boldsymbol{e} |\!|\!| \leq |\!|\!| \hat{\boldsymbol{e}} |\!|\!| + C \|\hat{\boldsymbol{e}}\|_{\frac{1}{2},h} \tag{17}$$

holds, where $|\!|\!| \cdot |\!|\!|$ is the energy norm. Note that if $\hat{\boldsymbol{e}} = \boldsymbol{e} = \boldsymbol{0}$ on Γ_D, then $|\!|\!| \hat{\boldsymbol{e}} |\!|\!| = |\!|\!| \boldsymbol{e} |\!|\!|$.

3.2. The energy-norm a posteriori error estimator

The general idea to derive an implicit residual-type *a posteriori* error estimator is to solve an approximation of the (projected) error residual equation (15). This

usually requires higher-order trial and test spaces because of the Galerkin orthogonality and would be computationally too expensive if computed globally. Therefore, the (projected) error residual equation (15) is solved in subdomains of the elastic body Ω, which can be chosen in a meshfree method as the integration cells.

The trial space for the local problems in each of the n_i integration cells Ω_i is thus defined as $\mathcal{V}_{E,i} = \{\boldsymbol{v}|_{\Omega_i} \,;\, \boldsymbol{v} \in \mathcal{V}_E\}$. Likewise, the local test space becomes $\mathcal{V}_i = \{\boldsymbol{v}|_{\Omega_i} \,;\, \boldsymbol{v} \in \mathcal{V}\}$. Consequently, the local bilinear form a_i on $\mathcal{V}_i \times \mathcal{V}_i$ is given by

$$a_i(\hat{\boldsymbol{e}}|_{\Omega_i}, \boldsymbol{v}) = \int_{\Omega_i} \boldsymbol{\sigma}(\hat{\boldsymbol{e}}|_{\Omega_i}) : \boldsymbol{\varepsilon}(\boldsymbol{v}) \, \mathrm{d}V. \tag{18}$$

Similarly, the local extended residual $\hat{R}_i$ on $\mathcal{V}_i$ reads

$$\hat{R}_i(\boldsymbol{v}) = \int_{\Omega_i} \boldsymbol{f}|_{\Omega_i} \cdot \boldsymbol{v} \, \mathrm{d}V + \sum_{l=1}^{n_l} \int_{E_l \subset \partial\Omega_i} \boldsymbol{t}_l \cdot \boldsymbol{v} \, \mathrm{d}A - \int_{\Omega_i} \boldsymbol{\sigma}(\boldsymbol{u}_h|_{\Omega_i}) : \boldsymbol{\varepsilon}(\boldsymbol{v}) \, \mathrm{d}V, \tag{19}$$

where n_l is the number of edges E_l of an integration cell and $\boldsymbol{t}_l = \boldsymbol{\sigma}(\boldsymbol{u}|_{\Omega_i}) \cdot \boldsymbol{n}$ are the exact tractions if $E_l \not\subset \Gamma_D$, otherwise $\boldsymbol{t}_l = \boldsymbol{\sigma}(\boldsymbol{u}_h|_{\Omega_i}) \cdot \boldsymbol{n}$ are the RKPM tractions.

With the above local forms (18) and (19) at hand, the projected discretization error restricted to an integration cell, i.e. $\hat{\boldsymbol{e}}|_{\Omega_i}$, satisfies the local form of the (projected) error residual equation (15) given as

$$a_i(\hat{\boldsymbol{e}}|_{\Omega_i}, \boldsymbol{v}) = \hat{R}_i(\boldsymbol{v}) \quad \forall \boldsymbol{v} \in \mathcal{V}_i. \tag{20}$$

Note that this a pure Neumann problem for each integration cell Ω_i. However, the extended residual $\hat{R}_i$ involves the generally unknown traction field $\boldsymbol{t}_l$. Therefore, we replace the exact tractions $\boldsymbol{t}_l$ in (19) by a computable traction field on each edge of the integration cell $E_l \subset \partial\Omega_i$, denoted by $\tilde{\boldsymbol{t}}_{l,h}$. The residual (19) then turns into

$$\tilde{R}_i(\boldsymbol{v}) = \int_{\Omega_i} \boldsymbol{f}|_{\Omega_i} \cdot \boldsymbol{v} \, \mathrm{d}V + \sum_{l=1}^{n_l} \int_{E_l \subset \partial\Omega_i} \tilde{\boldsymbol{t}}_{l,h} \cdot \boldsymbol{v} \, \mathrm{d}A - \int_{\Omega_i} \boldsymbol{\sigma}(\boldsymbol{u}_h|_{\Omega_i}) : \boldsymbol{\varepsilon}(\boldsymbol{v}) \, \mathrm{d}V. \tag{21}$$

From the requirement that the sum of the local residuals over all integration cells should match the global residual, it follows that $\tilde{\boldsymbol{t}}_{l,h}$ need to be compatible between the integration cells and that they need to fulfill the Neumann boundary conditions. The first requirement is already fulfilled by the RKPM tractions and the second requirement is obviously trivial to fulfill.

Replacing $\hat{R}_i$ by the computable residual $\tilde{R}_i$ in the local error residual equation (20) then yields the local problem

$$a_i(\boldsymbol{\psi}_i, \boldsymbol{v}) = \tilde{R}_i(\boldsymbol{v}) \quad \forall \boldsymbol{v} \in \mathcal{V}_i, \tag{22}$$

which we solve for a solution $\boldsymbol{\psi}_i \in \mathcal{V}_{E,i}$ that can be seen as an approximation of $\hat{\boldsymbol{e}}|_{\Omega_i}$ depending on the accuracy of the tractions $\tilde{\boldsymbol{t}}_{l,h}$. However, as mentioned above, (22) is

a pure Neumann problem. The solvability of (22) thus requires that the computable tractions $\tilde{\boldsymbol{t}}_{l,h}$ are also equilibrated, which results in additional computational efforts.

The summation of the local problems (22) over all n_i integration cells and subsequent application of the Cauchy-Schwarz inequality then yields the constant-free energy-norm estimator for the projected discretization error

$$\|\!|\hat{\boldsymbol{e}}|\!\| \leq \left(\sum_{n_i} a_i(\boldsymbol{\psi}_i, \boldsymbol{\psi}_i) \right)^{\frac{1}{2}}, \tag{23}$$

which bears resemblance to its finite element counterpart as originally introduced by Bank & Weiser [6] and Ainsworth & Oden [1].

From (17) we then immediately infer that the discretization error $\boldsymbol{e}$, measured in the energy norm, can be bounded from above as

$$\|\!|\boldsymbol{e}|\!\| \leq \left(\sum_{n_i} \eta_i \right)^{\frac{1}{2}} + C \left(\sum_{E_l \subset \Gamma_D} h_E^{-1} \eta_E \right)^{\frac{1}{2}}. \tag{24}$$

Here, $\eta_i = a_i(\boldsymbol{\psi}_i, \boldsymbol{\psi}_i)$ is the error estimator in the domain and $\eta_E = \|\hat{\boldsymbol{e}}\|^2_{L_2(E)}$ is the computable error on the Dirichlet boundary Γ_D.

Note that, in general, it is not required that the local problems (22) are solved with the same numerical method as used to approximate the model problem (3). Since the local problems are Neumann problems, the finite element method or RKPM can both be used with a sufficiently high polynomial order.

4. Goal-oriented a posteriori error estimation

For the practical engineer, further error measures than the energy norm are often of bigger interest, e.g. the error of the fracture criterion within the framework of linear elastic fracture mechanics (LEFM), see Stone & Babuška [13]. In the terminology of goal-oriented error estimation, the fracture criterion is an example of a quantity of interest and our aim is to control the error of such quantities of interest. The derivation of the goal-oriented error estimator follows the well-established duality strategy as originally elaborated by Eriksson et al. [9] and others.

4.1. The dual problem based on a multi-space approach

Let the quantity of interest be given by the linear or linearized functional Q defined on $\mathcal{V}_0$. Then the dual problem of (3) asks to find a solution $\overset{*}{\boldsymbol{u}} \in \mathcal{V}_0$ such that

$$a(\boldsymbol{v}, \overset{*}{\boldsymbol{u}}) = Q(\boldsymbol{v}) \quad \forall \boldsymbol{v} \in \mathcal{V}_0. \tag{25}$$

Note that since the linear elasticity problem is self adjoint, a is symmetric and thus (25) results from the primal problem (3) by simply replacing the right-hand side.

For the associated meshfree RKPM discretization of the above dual problem (25), we introduce the finite-dimensional subspace $\overset{*}{\mathcal{V}}_h \subset \mathcal{V}$. In the most general case, $\overset{*}{\mathcal{V}}_h$ is different from $\mathcal{V}_h$, which means that, compared to the discretization of the primal problem (3), we may use a different set of particles and even different RK shape functions for the Galerkin approximation of the dual solution. The homogeneous Dirichlet boundary conditions (2a) are again weakly imposed using Nitsche's method, which results in the discrete problem of finding a solution $\overset{*}{\boldsymbol{u}}_h \in \overset{*}{\mathcal{V}}_h$ such that

$$a_h(\boldsymbol{v}_h, \overset{*}{\boldsymbol{u}}_h) = Q(\boldsymbol{v}_h) \quad \forall \boldsymbol{v}_h \in \overset{*}{\mathcal{V}}_h \tag{26}$$

with associated discretization error $\overset{*}{\boldsymbol{e}} = \overset{*}{\boldsymbol{u}} - \overset{*}{\boldsymbol{u}}_h$.

4.2. The goal-oriented error estimator

To estimate the error of the quantity of interest Q, the general strategy is to set $\boldsymbol{v} = \boldsymbol{e}$ in the dual problem (25). Note, however, that $\boldsymbol{v}$ is required to be in the space $\mathcal{V}_0$ in (25), whereas $\boldsymbol{e}$ is an element of $\mathcal{V}_E$. Similar to the error residual equation in Section 3.1, we therefore need to extend the dual problem (25) to the case where $\boldsymbol{v}$ can be chosen from $\mathcal{V}$, which results in

$$\begin{aligned} Q(\boldsymbol{e}) = a(\boldsymbol{e}, \overset{*}{\boldsymbol{e}}) &- \int_{\Gamma_D} \boldsymbol{e} \cdot \boldsymbol{\sigma}(\overset{*}{\boldsymbol{e}}) \cdot \boldsymbol{n} \, \mathrm{d}A - \int_{\Gamma_D} \overset{*}{\boldsymbol{e}} \cdot \boldsymbol{\sigma}(\boldsymbol{e}) \cdot \boldsymbol{n} \, \mathrm{d}A \\ &+ \hat{R}(\overset{*}{\boldsymbol{u}}_h) - \int_{\Gamma_D} \boldsymbol{e} \cdot \boldsymbol{\sigma}(\overset{*}{\boldsymbol{u}}_h) \cdot \boldsymbol{n} \, \mathrm{d}A. \end{aligned} \tag{27}$$

Note that the last two terms in (27) are exactly computable.

As can be observed from (27), the (extended) residual of the primal problem $\hat{R}$ needs to be computed in terms of the RKPM solution of the dual problem $\overset{*}{\boldsymbol{u}}_h$. This mainly requires to integrate the dual RKPM solution $\overset{*}{\boldsymbol{u}}_h$ using the integration cells Ω_i of the primal problem. Since the particles are independent from the mesh, this computation is "a piece of cake", as opposed to a mesh-based method, where the transfer of the solution from one mesh to the other mesh can be tedious, see [12] for more details in this respect.

The first three terms on the right-hand side of (27) can now be estimated using the Cauchy-Schwarz inequality and an inverse estimate, see [11]. If the dual discretization is kept constant during adaptive refinements, then we arrive at the error estimate

$$|Q(\boldsymbol{e})| \leq C_1 |\!|\!| \hat{\boldsymbol{e}} |\!|\!| + C_2 \|\hat{\boldsymbol{e}}\|_{\frac{1}{2},h} + |R(\overset{*}{\boldsymbol{u}}_h) - \int_{\Gamma_D} \boldsymbol{e} \cdot \boldsymbol{\sigma}(\overset{*}{\boldsymbol{u}}_h) \cdot \boldsymbol{n} \, \mathrm{d}A|, \tag{28}$$

where the positive constants C_1 and C_2 include several constants. The first term in the above estimate can be estimated using the energy-norm error estimator (23).

If, in addition, the errors on the Dirichlet boundary vanish, this estimate can be simplified even further to

$$|Q(\boldsymbol{e})| \leq C_1 |\!|\!| \hat{\boldsymbol{e}} |\!|\!| + |R(\overset{*}{\boldsymbol{u}}_h)| \tag{29}$$

with constant $C_1 = |\!|\!| \overset{*}{\hat{\boldsymbol{e}}} |\!|\!|$.

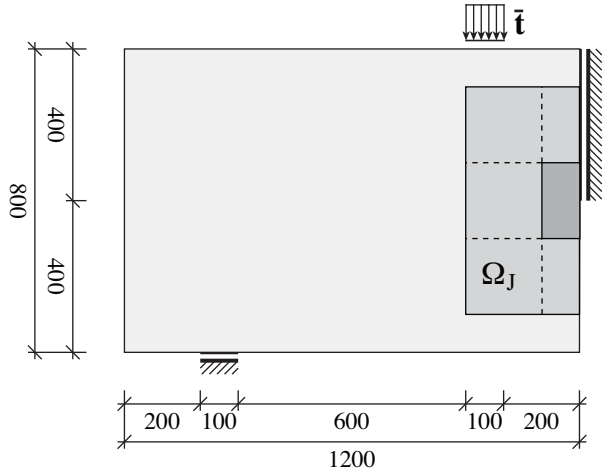

Figure 1: System and loading, measurements in mm

Figure 2: Primal error distribution

Figure 3: Dual error distribution

5. Numerical example: 4-point bending

In this section, we aim at investigating the goal-oriented error estimator for the case of the J-integral as an example for a nonlinear quantity of interest in LEFM. In a material force setting within Eshelbian mechanics, the J-integral takes the form

$$J(\boldsymbol{u}) = -\int_{\Omega_J} \boldsymbol{\Sigma}(\boldsymbol{u}) : \boldsymbol{H}(q\bar{\boldsymbol{x}})\, \mathrm{d}A. \tag{30}$$

Here, q is a C^0-function with $q = 1$ at the crack tip and $q = 0$ on $\Gamma_J = \partial\Omega_J \setminus \Gamma_c$. Moreover, $\boldsymbol{H}(\cdot) = \boldsymbol{\nabla}(\cdot)$ is the gradient tensor and $\boldsymbol{\Sigma} = W_s \boldsymbol{I} - \boldsymbol{H}^T \cdot \boldsymbol{\sigma}$ is the Newton-Eshelby stress tensor with the specific strain-energy function $W_s = 1/2\boldsymbol{\varepsilon} : \mathbb{C} : \boldsymbol{\varepsilon}$ and the identity tensor $\boldsymbol{I}$. The linearized quantity of interest Q is then defined as

$$Q(\boldsymbol{v}) = -\int_{\Omega_J} \boldsymbol{\Sigma}_{\mathrm{lin}}(\boldsymbol{u}_h) : \boldsymbol{H}(\boldsymbol{v})\, \mathrm{d}A, \tag{31}$$

where we introduced the linearized stress tensor

$$\boldsymbol{\Sigma}_{\mathrm{lin}}(\boldsymbol{u}_h) = \mathrm{div}(q\bar{\boldsymbol{x}})\boldsymbol{\sigma}(\boldsymbol{u}_h) - \boldsymbol{\sigma}(\boldsymbol{u}_h) \cdot \boldsymbol{H}^T(q\bar{\boldsymbol{x}}) - \boldsymbol{H}(q\bar{\boldsymbol{x}}) : \left[\boldsymbol{H}^T(\boldsymbol{u}_h) \cdot \mathbb{C}\right]. \tag{32}$$

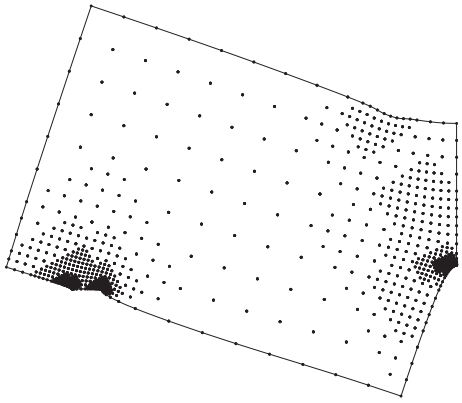

Figure 4: Adaptive primal refinement

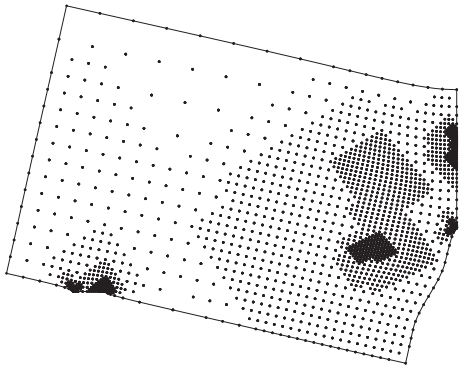

Figure 5: Adaptive dual refinement

The system in this example is a pre-cracked glass plate in plane-stress state subjected to 4-point bending, as illustrated in Figure 1. The material data is given in terms of Young's modulus $E = 64.000$ N/mm^2 and Poisson's ratio $\nu = 0.2$. The load in this example is $|\bar{\boldsymbol{t}}| = 1$ N/mm^2. The reference value $J(\boldsymbol{u}) = 0.016186862$ kJ/m^2 was computed using an adaptively refined Q_2 finite element mesh with 2.434.140 degrees of freedom (for the discretized half of the system).

As can be seen, the linearization depends on the solution of the primal problem. Therefore, one needs to solve the primal problem, use its solution to create the load of the dual problem, solve the dual problem and use the solution of both the primal and the dual problem to estimate the error of the J-integral. These steps can be easily carried out using the proposed multi-space RKPM approach.

In Figs. 2 and 3 the distribution of the exact error in each integration cell is visualized for both the primal and the dual problem (darker areas indicate larger errors). Accordingly, it can be expected that the error estimator finds the regions and refines the particles where large errors appear. This can be verified in terms of the 13-*th* primal refinement and 10-*th* dual refinement, see Figs. 4 and 5, respectively.

A comparison of various methods to deal with the dual problem is plotted in Figs. 6 and 7. It can be observed that the convergence rate is decreased when the dual discretization remains constant, which becomes clear from the error estimate (28). It can also be seen that when a fine dual discretization is used, the error is much smaller and thus the error tolerance could be reached with far less refinement steps compared to the other cases. A coarse and constant dual discretization, on the other hand, has the advantage of being computationally inexpensive. For a higher convergence rate, especially in the case of adaptive refinements, it is recommendable to refine both the primal and the dual discretization. The presented multi-space approach allows in this case to refine both problems independently and conveniently, which is not straightforwardly possible using a mesh-based method. Moreover, the refinement process itself is much easier using a meshfree method, because particles can be easily added and even removed from the discretization.

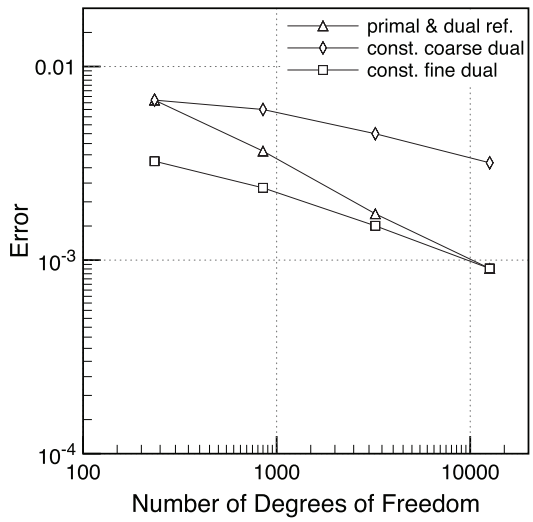

Figure 6: Estimated error $Q(\boldsymbol{e}) \approx J(\boldsymbol{u}) - J(\boldsymbol{u}_h)$, uniform refinements

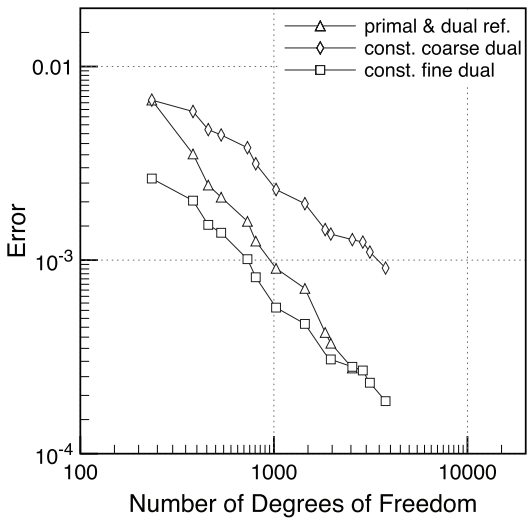

Figure 7: Estimated error $Q(\boldsymbol{e}) \approx J(\boldsymbol{u}) - J(\boldsymbol{u}_h)$, adaptive refinements

6. Conclusions

In this paper, both an implicit energy-norm and a goal-oriented *a posteriori* error estimator for RKPM approximations were derived and implemented. As it turned out, the main problem in the derivation of the error estimator is the violation of Dirichlet boundary conditions in meshfree methods. To cope with this problem, a projected error and thus a projected error residual equation were introduced. Since the RKPM particles are independent from the integration cells, a multi-space approach could easily be established allowing to use different discretizations for the primal and the dual problem. The error estimator was successfully applied to the J-integral as a crack propagation criterion in LEFM, offering the possibility to use only one (coarse or fine) dual solution within the refinement scheme and thus either obtaining less accurate but inexpensive (for the coarse solution) or more accurate but also more expensive (for the fine solution) error estimates.

Acknowledgements

The support of this work by DFG (German Research Foundation) under the grant no. RU 1213/2-1 is very much appreciated.

References

[1] Ainsworth, M. and Oden, J. T.: *A posteriori error estimation in finite element analysis*. John Wiley & Sons, New York, 2000.

[2] Babuška, I., Banerjee, U., and Osborn, J.: Survey of meshless and generalized finite element methods: A unified approach. Acta Numer. (2003), 1–125.

[3] Babuška, I. and Rheinboldt, W. C.: A-posteriori error estimates for the finite element method. Int. J. Numer. Meth. Engng **12** (1978), 1597–1615.

[4] Babuška, I. and Rheinboldt, W. C.: Error estimates for adaptive finite element computations. SIAM J. Numer. Anal. **15** (1978), 736–754.

[5] Babuška, I. and Strouboulis, T.: *The finite element method and its reliability.* Oxford University Press, Oxford, 2001.

[6] Bank, R. E. and Weiser, A.: Some a posteriori error estimators for elliptic partial differential equations. Math. Comp. **44** (1985), 283–301.

[7] Chen, J. S., Pan, C., Wu, C. T., and Liu, W. K.: Reproducing Kernel Particle Methods for large deformation analysis of non-linear structures. Comput. Methods Appl. Mech. Engrg. **139** (1996), 195–227.

[8] Duarte, C. A. and Oden, J. T.: An *h-p* adaptive method using clouds. Comput. Methods Appl. Mech. Engrg. **139** (1996), 237–262.

[9] Eriksson, K., Estep, D., Hansbo, P., and Johnson, C.: Introduction to adaptive methods for differential equations. Acta Numer. (1995), 106–158.

[10] Nitsche, J. A.: Über ein Variationsprinzip zur Lösung von Dirichlet-Problemen bei Verwendung von Teilräumen, die keinen Randbedingungen unterworfen sind. Abh. Math. Semin. Univ. Hambg. **36** (1971), 9–15.

[11] Rüter, M. and Chen, J. S.: A goal-oriented error estimator for meshfree methods based on a multi-space approach. (Submitted to Comput. Methods Appl. Mech. Engrg.) (2015).

[12] Rüter, M., Korotov, S., and Steenbock, C.: Goal-oriented error estimates based on different FE-spaces for the primal and the dual problem with applications to fracture mechanics. Comput. Mech. **39** (2007), 787–797.

[13] Stone, T. J. and Babuška, I.: A numerical method with a posteriori error estimation for determining the path taken by a propagating crack. Comput. Methods Appl. Mech. Engrg. **160** (1998), 245–271.

[14] Vidal, Y., Parés, N., Díez, P., and Huerta, A.: Bounds for quantities of interest and adaptivity in the element-free Galerkin method. Int. J. Numer. Meth. Engng. **76** (2008), 1782–1818.